Chronic social stress in mice alters energy status including higher glucose need but lower brain utilization

Simone Carneiro-Nascimento[1], Jolanta Opacka-Juffry[1], Adele Costabile[1], Christina N. Boyle[2], Adrienne Müller Herde[3], Simon M. Ametamey[3], Hannes Sigrist[4], Christopher R. Pryce[4]*, Michael Patterson[1]*

1 Department of Life Sciences, University of Roehampton, London, UK

2 Institute of Veterinary Physiology, University of Zurich, Zurich, Switzerland

3 Center for Radiopharmaceutical Sciences, Swiss Federal Institute of Technology Zurich, Zurich, Switzerland

4 Preclinical Laboratory for Translational Research into Affective Disorders, Department of Psychiatry, Psychotherapy & Psychosomatics, University of Zurich, Zurich, Switzerland

*CR Pryce and M Patterson contributed equally to this work

Corresponding authors: Dr. Michael Patterson, Department of Life Sciences, University of Roehampton, London, UK. Michael.Patterson@roehampton.ac.uk and Prof. Christopher R Pryce, Preclinical Laboratory for Translational Research into Affective Disorders, Department of Psychiatry, Psychotherapy & Psychosomatics, University of Zurich, Zurich, Switzerland, christopher.pryce@bli.uzh.ch

Abstract

Chronic stress leads to changes in energy status and is a major risk factor for depression, with common symptoms of reductions in body weight and effortful motivation for reward. Indeed, stress-induced disturbed energy status could be a major aetio-pathogenic factor for depression. Improved understanding of these putative inter-relationships requires animal model studies of effects of stress on both peripheral and central energy-status measures and determinants. Here we conducted a study in mice fed on a standard low-fat diet and exposed to either 15-day chronic social stress (CSS) or control handling (CON). Relative to CON mice, CSS mice had attenuated body weight maintenance/gain despite consuming the same amount of food and expending the same amount of energy at any given body weight. The low weight of CSS mice was associated with less white and brown adipose tissues, and with a high respiratory exchange ratio consistent with increased dependence on glucose as energy substrate. Basal plasma insulin was low in CSS mice and exogenous glucose challenge resulted in a relatively prolonged elevation of plasma glucose. With regard to hunger and satiety hormones, respectively, CSS mice had higher levels of acylated ghrelin in plasma and of ghrelin receptor gene expression in ventromedial hypothalamus and lower levels of plasma leptin, relative to CON mice. However, whilst CSS mice displayed this constellation of peripheral changes consistent with increases in energy need and glucose utilization relative to CON mice, they also displayed attenuated uptake of [^{18}F]FDG in brain tissue specifically. Reduced brain glucose utilization in CSS mice could contribute to the reduced effortful motivation for reward in the form of sweet-tasting food that we have reported previously for CSS mice. It will now be important to utilize this model to further understanding of the mechanisms via which chronic stress can increase energy need but decrease brain glucose utilization and how this relates to regional and cellular changes in neural circuits for reward processing relevant to depression.

Keywords: Mouse model, stress, body weight, energy, calorimetry, brain glucose uptake

1. Introduction

Chronic stress leads to a constellation of changes in physiological systems that require energy and it impacts markedly on energy status e.g. balance and metabolism (Harris, 2014). Chronic stress is also a major risk factor for depression (Kessler, 1997), and disturbed energy metabolism, particularly in the glucose-demanding central nervous system (CNS), is proposed as a major aetio-pathogenic cause of depression (Harper et al., 2017). Indeed, depression includes reduced interest in daily activities, measured as attenuated effortful motivation, as a core symptom, and either loss or gain of body weight, possibly accompanied by a corresponding appetite change, as a common symptom (American Psychiatry Association, 2013). Also, in non-depressed individuals, most studies report that (perceived) stress leads to appetite change, and this can be either appetite loss or gain (Torres and Nowson, 2007). Stress and depression are associated with altered peripheral levels of regulators of energy homeostasis, a number of which enter the CNS to bind to their receptors and thereby modulate the neural circuitry of feeding behavior/food intake (Simmons et al., 2018). It is possible that chronic stress leads to disrupted energy status and, causally unrelated to this, co-morbid depression; but it is also possible that chronic stress disrupts energy status, which then in turn contributes causally to depression. Improved understanding of these putative inter-relationships and their underlying mechanisms is imperative, and relevant psychoneuroendocrine animal models in which the effects of specific chronic stressors on both peripheral and central measures of energy status are investigated, are essential in this regard.

Homeostatic energy-regulation systems constitute a complex network of peripheral and central signals. They include the neuroendocrine systems that relay signals between periphery and CNS (Farias et al., 2017). Ghrelin, released from the stomach, is a hunger hormone and can stimulate feeding (Müller et al., 2015). Ghrelin levels are high in preprandial periods and suppressed following a meal (Cummings et al., 2001). Its receptor, growth hormone secretagogue receptor (Ghs-r1a), is expressed in numerous tissues including CNS (Cong et al., 2012). Conversely, leptin, an adipokine, is released from adipose tissue and acts at central receptors, primarily in the hypothalamus, to suppress feeding, and to increase energy expenditure and signal long-term energy stores (Friedman, 2014). Both ghrelin and leptin can be altered in depression. Ghrelin is increased in depression and is proposed to contribute to stress-related eating (Bali and Jaggi, 2016); for leptin, studies report either lower or higher circulation in depression

(Joung et al., 2014; Lu, 2007). The hormone insulin is synthesized in the pancreas and facilitates both the utilization of glucose to produce energy and glucose storage. Depression is associated with a mild increase in insulin resistance (Kan et al., 2013).

In rodents, there is evidence that chronic stress leads to changes in both peripheral and central energy status and their regulation. There are several reports that chronic stress leads to increased daily food intake without an effect on body weight, suggesting that greater energy intake is accurately reflecting increased energy need. This has been observed in mice using 10 days of chronic social defeat (CSD) (Moles et al., 2006; Kumar et al., 2013), and a similar procedure of chronic social stress (CSS) that is maintained for 15 days (Bergamini et al., 2016; Kukelova et al., 2018). There are also reports that chronic stress leads to increases in both food intake and body weight (Chuang et al., 2010; Razzoli et al., 2011). Using indirect calorimetry, mice exposed to 24-day CSS were demonstrated to display an increase in energy expenditure (Coccurello et al., 2017). Recently, mouse CSS and CSD were reported to induce hyperglycemia in blood and brain and to do so without affecting insulin sensitivity (Sanghez et al., 2013; Van Der Kooij et al., 2018). Interestingly, this co-occurred with reduced whole-brain glucose uptake (Van Der Kooij et al., 2018). Plasma ghrelin is increased in CSD mice (Chuang et al., 2011; Kumar et al., 2013) and plasma leptin is reduced in CSD and CSS mice (Bergamini et al., 2016; Chuang et al., 2010). Whilst both of these endocrine effects of chronic stress would be expected to lead to increased food intake, this would also depend on any effects on central levels of receptors for these hormones; for example, CUMS rats displayed decreased hypothalamic expression of the leptin receptor (Ge et al., 2013).

Concerning the link to depression, rodent chronic stressor manipulations have been combined with behavioral tests of responding for sweet food, to model the core symptom of reduced reward interest. Several weeks of chronic unpredictable mild stress (CUMS) in rats and 10-day CSD in mice lead to reduced preference for sucrose or saccharin versus water in a choice test (Krishnan et al., 2007; Willner, 2017). The 15-day CSS procedure in mice leads to reduced Pavlovian learning that a neutral stimulus predicts sucrose and reduced effortful motivation to earn sucrose (Bergamini et al., 2016; Kúkel'ová et al., 2018). Therefore, there is translational evidence that chronic stress leads to reduced interest in reward in the form of sweet-tasting food, even though there is an increase in daily food intake.

In this study, the overall aim was to conduct a thorough investigation of the effects of CSS on peripheral and central measures of energy status in mice maintained on a standard low-fat diet. In a first experiment, we conducted a detailed assessment of the effects of mouse CSS on body weight, food intake, energy expenditure and energy source, and white and brown adipose tissue mass. In a second experiment, the effects of CSS on plasma insulin levels and glucose homeostasis, and on plasma levels of ghrelin and leptin and the central gene expression of their receptors, were studied. In a third experiment, the effect of CSS on glucose ([^{18}F]FDG) uptake by peripheral organs/tissues and by brain were investigated. We identified a constellation of peripheral changes consistent with CSS leading to changes in energy status, e.g. CSS mice had similar food intake and energy expenditure but lower body weight gain relative to controls, and glucose utilization, e.g. CSS mice had a higher respiratory exchange ratio than controls. Interestingly, however, these CSS effects co-occurred with decreased glucose utilization by the brain specifically. Together, these findings demonstrate the importance of understanding the complex effects of chronic stress on peripheral and central energy status, and how can provide insights into the relevance of stress-induced changes in energy status for depression.

2. Methods

2.1 Animals and housing

Male C57BL/6J (BL/6) mice were bred in-house and weaned at age 3 weeks, when they were caged in groups of 2-3 littermates. At experiment onset, they were aged 10-13 weeks and weighed 24.0-30.0 g. Male CD-1 mice (Janvier, Saint-Berthevin, France) used in the chronic social stress manipulation were 8 months, ex-breeders and caged singly. Cages were type 2L (33 x 21 x 14 cm) and individually ventilated at 22-24 °C and 50-60% humidity, and contained sawdust and paper tissue as nesting material. Mice were maintained on a reversed 12:12 h light-dark cycle with lights off 07:00-19:00 h. They were provided with ad libitum standard complete-pellet diet (Kliba Nafag, Granovit): dry matter 88%, crude protein 18.5%, crude fat 4.5%. Water was also available ad libitum. The study was conducted under permits for animal experimentation (170/2012, 149/2015) issued by the Veterinary Office of Zurich. The number of mice studied was the minimum necessary to achieve the study aims and all unnecessary stress was avoided.

2.2 Experimental design

Three iterative experiments were conducted, the designs of which are presented in Figure S1. In Expt 1, food intake was measured and indirect calorimetry carried out with 12 CSS and 12 control (CON) mice, to investigate energy expenditure and respiratory exchange ratio. Interscapular brown adipose tissue (iBAT), epididymal white adipose tissue (eWAT) and the brain were collected for determination of gene expression of neuroendocrine appetite regulators. Expt 2, conducted with 12 CSS and 12 CON mice, investigated effects of stress by day 10 of the CSS procedure on blood levels of glucose and plasma insulin in the fasted basal state and in a glucose tolerance test, and effects of CSS on fasting plasma levels of insulin and appetite hormones at day 17. In Expt 3, conducted with 7 CSS and 7 CON mice, an ex vivo biodistribution study of 2-[^{18}F]-fluoro-D-desoxy-D-glucose was conducted on day 16. The sample size of N=12 per group used in Expts 1 and 2 was the same as that used to identify effects of CSS on physiology (e.g. Azzinnari et al., 2014), neurobiology (e.g. Grandjean et al., 2016) and behavior (e.g. Bergamini et al., 2018). The sample size of N=7 per group used in Expt 3 allowed all mice to be studied within 1 day with the same production of [^{18}F]FDG; it was informed by a study of CSD effects on [^{18}F]FDG brain uptake in which a sample size of N=8-9 was sufficient to identify an effect on cerebral glucose uptake (Van Der Kooij et al., 2018).

2.3 Chronic social stress

The CSS procedure is described in detail in Azzinnari et al. (2014). The home cages of aggressive CD-1 mice were divided longitudinally into two compartments using transparent, perforated Plexiglas. To prevent bite wounds, the lower incisors of CD-1 mice were trimmed every third day. On CSS day 1, the experimental mouse was placed in the same compartment as a CD-1 mouse and behavior was observed: the intruder and resident were maintained together for either 10 min or 60 s cumulative attack time, whichever occurred sooner. The CD-1 mouse was then transferred to the adjacent compartment of its cage and the two mice were maintained in sensory contact for 24 h. On each of days 2-15, the CSS – CD-1 mouse pairings were rotated and the above procedure repeated, so that each CSS mouse was placed together with at least 12 different CD-1 mice. Each CSS mouse was observed to be attacked by each CD-1 mouse with attacks comprising chase, box and bite behaviors by CD-1 mice; the duration of daily attacks was 59 ± 1 s, 48 ± 6 s and 49 ± 3 s (overall daily mean ± SD) for CSS mice in Expts 1, 2

and 3, respectively. In addition to actively attempting to avoid and escape from CD-1 mice, the behavior of CSS mice included the submissive behaviors of upright and horizontal freezing and vocalization; however, these submissive acts did not defer attacks by the CD-1 mice, such that CSS mice experienced daily defeat by an uncontrollable social stressor. Control mice were handled and weighed on each of days 1-15. With respect to CON mice, in Expt 2 they remained in littermate pairs (Azzinnari et al., 2014), and in Expt 1 and Expt 3 they were single-housed such that the thermal and psychological stress of single housing (Gordon et al., 1998) were similarly present for CSS and CON mice.

2.4 Body weight and food intake

In each experiment, body weight (BW) of BL/6 mice was measured daily at 14:00 h. In Expt 1, daily food intake was measured by weighing three food pellets, placing them inside the home cage, and weighing the remainder 24 h later. (Using metabolic cages, we observed that 1-3% of the pellet weight eaten was lost onto the cage floor as "dust" thereby leading to a small but consistent over-estimate of pellet consumption.). The per mouse mean daily BW and food intake were calculated per 5-day block. The overall change in BW relative to food intake, measured as (BW at day 20 minus BW at day -4)/(total food intake on CSS/CON days -4 to 20), was also calculated for each mouse in Expt 1.

2.5 Indirect calorimetry for energy expenditure and respiratory exchange ratio

In Expt 1, indirect calorimetry was conducted during 5 days prior to (baseline) and 5 days after CSS/CON. An automated open-circuit indirect calorimetry system (Type III, PhenoMaster Home Cage, TSE Systems) was used to investigate CSS effects on energy expenditure and the nutrient-substrate source of the energy produced. Each mouse was placed in a gas-tight metabolic cage containing food pellets and a water bottle. The ambient temperature and humidity were maintained at 23.4 ± 0.2°C and 54.7 ± 6%, respectively. In the system, each cage was connected to a fresh air supply, which also provided the sample switch unit for drawing air samples, measuring the flow rate and analyzing the gas concentration of the incoming and outgoing air for oxygen (O_2) and carbon dioxide (CO_2). Every 20 min, measurements were obtained for O_2 consumption and CO_2 production and, from these, energy expenditure (EE) and respiratory exchange ratio (RER) were derived; average hourly values were calculated. EE is derived from the volume of O_2 consumed for energy metabolism. EE increases with BW, and therefore to control appropriately for the relatively low BW observed in CSS compared with

CON mice (see Results), EE KJ/h data were analyzed with analysis of covariance using BW as covariate. That is, the effect of BW and any additional effect of CSS at any given BW were analyzed (Tschöp et al., 2012). RER is the ratio of CO_2 produced and O_2 consumed in energy metabolism (Arch et al., 2006). RER provides an indirect estimate of substrate utilization: 0.7 indicates predominate lipid utilization and 1.0 predominate carbohydrate utilization. (Ferrannini, 1988; Arch et al., 2006). During the baseline period (days -4 to 0), the first 3 days were used to acclimatize mice to the metabolic cages, and the data collected on days -1 and 0 specifically were used for the analysis. After CSS/CON, day 16 was used to re-acclimatize mice and the data collected on days 17-20 were used for analysis.

2.6 Behavioral measurement

In Expt 1, spontaneous behaviors in the home cage were measured using an ethogram comprising 10 behaviors: eating, drinking, self-grooming, foraging, sitting upright, resting, "at divider", locomoting, climbing, and rearing. On each of CSS/CON days 4, 8 and 12, a 1-h observation was conducted at each of 8-9:00 h, 11-12:00 h, 16-17:00 h and 19-20:00 h. The method of instantaneous scan sampling was applied, whereby each mouse was observed in turn for 10 sec every 2 min (30 sample points per hour per mouse), and the predominant behavior during each 10 sec sample was scored (Martin and Bateson, 2007).

2.7 Glucose tolerance test

In Expt 2, mice were fasted from 18:00 h on day 9 until completion of sampling on day 10 of the CSS/CON procedure. Starting at 08:00 h on day 10, a baseline blood sample was collected (time -1 min) followed immediately (time 0 min) by intraperitoneal injection of a 20% (W/V) β-D-glucose (Sigma) solution in PBS as 2 mg/10 μL/g BW (Bowe et al., 2014). Blood samples were then drawn at times 15, 30, 45, 60 and 120 min. For each blood sample, the mouse was placed inside a restraint tube for 1-2 min. The tail protruded from the restraint tube and was held next to and warmed with an infrared lamp. For the first blood sample a 1-2 mm incision was made on the lateral surface of the tail tip and 50 μL blood were collected into an EDTA coated capillary tube (Microvette, Sarstedt); all subsequent samples were collected from the same incision site. Immediately after each blood sampling the mouse was removed from the restraint tube and returned to its home cage. Blood samples were placed on ice. At each sampling time point, an additional 20 μL blood was collected on a test strip for measurement

of blood glucose concentration using a hand-held blood glucose meter (ACCU-CHEK Aviva, Roche). After completion of the final blood sampling, mice were given ad libitum food again. Blood samples were centrifuged for 10 min at 780 g and 4˚C, and the plasma transferred to cryotubes (Protein LoBind, Eppendorf) and stored at -80˚C. Insulin concentration was determined using the Mouse Insulin ELISA kit (#90080, CrystalChem) according to the manufacturer's protocol. The sensitivity range of the assay based on 5 µL plasma was 0.1-6.4ng/mL using duplicate determinations.

2.8 ELISAs for plasma ghrelin and leptin

On day 20 in Expt 1 and on day 16 in Expt 2, mice were fasted overnight in order to allow for analysis of appetite hormones under the same conditions across mice. On the following day, at 09-10:00 h, trunk blood was collected into 500 µL EDTA-coated tubes (Microvette, Sarstedt). For the assay of active ghrelin, 100 µL of each blood sample was subsequently transferred into a second tube (Microvette, Sarstedt) containing the esterase inhibitor 4-2-aminoethyl-benzenesulfonyl fluoride (Sigma) at a final concentration of 1 mg/mL. Blood was centrifuged for 10 min at 780 g and 4°C, and plasma aliquots were transferred to cryotubes (Eppendorf, Protein LoBind). In the case of the samples for active ghrelin, hydrochloric acid (Merck Millipore) was added to give a final concentration of 0.05 N. Plasma samples were stored at -80°C. Plasma acylated active ghrelin (Rat/Mouse Ghrelin (active) EZRGRA-90K, Merck Millipore) and plasma leptin (Mouse Leptin #90030, CrystalChem) were measured using ELISA kits, in accordance with the manufacturers' protocols. For plasma active ghrelin, assay sensitivity based on 20µL was 8 pg/mL, with duplicate determinations; for plasma leptin, assay sensitivity based on 5 µL was 0.2-12.8 ng/mL, with duplicate determinations.

2.9 Tissue collection

In Expt 1, on day 21, directly after trunk blood sampling, the brain was removed from the skull and frozen in isopentane at -40°C followed by storage at -80°C. Epididymal WAT and iBAT were carefully dissected out and weighed, and then frozen on dry ice followed by storage at -80°C.

2.10 Real-time quantitative PCR of gene expression in fat tissue and brain

In Expt 1, from 30 mg iBAT and 50-100 mg eWAT, total RNA was isolated using the RNeasy Lipid Tissue Mini Kit (Qiagen), and further digested with DNase I (Qiagen). For both iBAT and eWAT, 200 ng RNA were used: in iBAT the gene of interest was uncoupling protein 1 (*Ucp-1*) and in eWAT the

genes of interest were leptin (*Lep*) and leptin receptor (*Lepr*). Frozen brains were embedded in optimal cutting temperature compound (Scigen, USA) and cut coronally into 300 µm sections on a cryostat (Bright) at -18˚C. Regions of interest were medial prefrontal cortex (mPFC), nucleus accumbens (NAcc), paraventricular nucleus including periventricular nucleus of the hypothalamus (PVN), arcuate nucleus of the hypothalamus (ARC), ventromedial nucleus of the hypothalamus (VMH) and ventral tegmental area (VTA). Using the cryostat at a chamber temperature of -24˚C, these regions were microdissected bilaterally from the corresponding sections using brain punchers (Ø=0.5 or 1 mm, model 57397, Stoelting) and by referring to a mouse brain atlas (Paxinos and Franklin, 2004). Total RNA was extracted from micro-punched tissue using the RNeasy Micro Kit (Qiagen). Depending on the RNA yield for each brain region, different amounts of RNA were used (27-60 ng). The genes of interest were the ghrelin receptor (*Ghs-r1a*) in PVN, ARC, VMH and VTA, and *Lepr* in all regions. The RNA was reverse transcribed using the High Capacity cDNA Reverse Transcription Kit (Applied Biosystems). The housekeeping gene *Actb* was used for normalisation. Primer pairs for *Ucp-1, Lep a*nd *Actb* were designed using NCBI Primer-BLAST. The BLAST-Like Alignment Tool (UCSC Genome Browser) was used to check for primer sequence alignment. The primers were synthesized by Invitrogen (ThermoScientificTM). Predesigned KiCqStart® primer pairs (Sigma-Aldrich) were used for *Lepr* and *Ghs-r1a*. Primers details are given in Table S1. Specific quantification of cDNA targets was conducted using the QuantiFast SYBR Green PCR Kit (Qiagen). The PCR cycle and annealing conditions used are given in Table S1.

2.11 Ex vivo glucose biodistribution study

In Expt 3, on day 16 starting at 08:00 h, mice were fasted for 1 hour to exclude effects of recent food intake, and then placed in a restraint tube with the tail immersed in water at 47°C for 30 sec. A 200 µl bolus of 2-[^{18}F]-fluoro-D-desoxy-D-glucose ([^{18}F]FDG) containing 24-27 MBq and estimated < 5 nmol 2-FDG was injected into the lateral tail vein and the mouse then placed into a metabolic cage. After 45 min the mouse was transferred to a chamber and anaesthetised for 30 sec with 4% isoflurane in an air: O_2 mixture at a flow rate of 700 ml/min prior to decapitation and trunk blood collection. Samples of tissues, including various brain regions, were collected and weighed, as described in Sephton et al. (Sephton et al., 2015). Radioactivity was measured in a gamma-counter (Wizard 1480, Perkin Elmer).

The accumulated radioactivity was expressed as the percentage of the normalised (MBq/kg BW) injected dose (ID) of [^{18}F]FDG per gram of tissue (% normalised ID/g tissue).

2.12 Statistical analysis

Statistical analysis of CSS effects was conducted using SPSS (version 24, SPSS Inc., Chicago IL, USA). For BW and change in BW relative to food intake, repeated measures analysis of covariance (ANCOVA) was conducted with pre-CSS/CON BW as covariate, and food intake was measured with ANOVA. Concerning indirect calorimetry, EE data were analyzed with ANCOVA using BW as covariate, whilst RER was independent of BW. Linear mixed models (LMMs) were used with dark and light circadian periods analyzed separately. Group (CSS, CON) and day (-1, 0, 17, 18, 19, 20) were fixed effects, with mean BW on these days as covariate in the case of EE; significant main or interaction effects were analyzed *post hoc* using Bonferroni correction. For home-cage behaviors, ANOVAs were conducted with between-subject factors of group, day and time, and to compensate for multiple testing significance was set at $p \leq 0.01$; significant main or interaction effects were analyzed *post hoc* using LSD. For blood glucose and plasma insulin, repeated measures ANCOVA was used with a between-subject factor of group and within-subject factor of time, and baseline glucose or insulin concentration as covariate; *post hoc* testing was conducted using LSD. Independent Student's *t*-tests were conducted for glucose and insulin area under the curve (AUC), iBAT mass, eWAT mass, plasma ghrelin and leptin. RT-PCR data were calculated as ΔCt mean ± SEM; analysis was carried out using the $2^{-\Delta\Delta Ct}$ method and *t*-tests. For [^{18}F]FDG uptake, CSS and CON mice were compared using *t*-tests with significance set at $p<0.01$ to compensate for multiple testing. Data are given as mean ± 1 SD. Unless stated otherwise above, statistical significance was set at $p \leq 0.05$.

3. Results

3.1 Effects of CSS on energy status and neuroendocrine regulators of feeding

3.1.1 Body weight, food intake and adipose tissue

In Experiment 1, body weight and food intake were measured from day -4 to day 20, i.e. from 5 days pre-CSD to 5 days post-CSD. There was an effect of CSS on body weight (Figure 1A): in ANCOVA

with baseline BW as covariate, there was a group x day block interaction effect ($F(2, 43)=11.9$, $p<0.0001$), with CSS mice weighing less than CON mice at days 11-15 and 16-20. Interestingly, this relatively low BW in CSS mice did not co-occur with any group difference in food intake (ANOVA: $p=0.45$, Figure 1B). The measure (change in BW)/(cumulative food intake) between day -4 and day 20 (Figure 1C) was significantly lower in CSS compared with CON mice ($t(22)=2.42$, $p<0.05$). At day 21, the eWAT and iBAT tissues were collected and weighed: CSS mice had significantly less eWAT mass than did CON mice ($t(22)=4.11$, $p<0.0001$, Figure 1D), and this was also the case for iBAT ($t(17)=5.99$, $p<0.0001$, Figure 1E).

(FIGURE 1 ABOUT HERE)

3.1.2 Energy expenditure and respiratory exchange ratio

On days -4 to 0 pre-CSD and 16 to 20 post-CSD, Expt 1 mice were placed in the indirect calorimetry chambers; after respective acclimatization periods, study data were collected on days -1 and 0 and days 17-20. Energy expenditure in kJ/h and RER were analyzed using a linear mixed model with fixed effects of group (CSS, CON) and day (-1, 0, 17, 18, 19 20), and separately for the dark and light phases of the circadian cycle. Given that BW was significantly lower in CSS mice than CON mice at days 16-20 (Fig. 1A), and given that EE will increase with BW, it was important to include BW as a covariate in the EE analysis. In the dark phase (Figure 2A), there was indeed a significant contribution of BW to EE (main effect: $F(1, 73.5)=27.12$, $p<0.0001$). Having controlled for BW, there was no additional significant effect of CSS on EE at any given BW (main effect of group: $p=0.07$). In the light phase (Figure 2A), there was again a significant main effect of BW on EE ($F(1, 64.0)=34.03$, $p<0.0001$), and again there was no additional significant effect of CSS on EE (main effect of group: $p=0.13$). The EE ANCOVA findings were similar when the analysis was restricted to post-CSD days 17-20 specifically: dark phase, BW $p<0.001$, group p=0-10; light phase, BW $p<0.0001$, group $p=0.09$. Therefore, at days 17-20 post-CSS/CON, CSS mice were eating a similar amount of food as and had a similar EE to CON mice at any given BW, but they were of lower BW than CON mice, indicating that CSS mice were expending a higher proportion of their energy on processes other than BW maintenance/gain. For RER, in ANCOVA there was no consistent association between BW and RER and therefore BW was not included as a covariate in the LMM. During the dark phase (Figure 2B), there was a group x day interaction effect

(F(5, 107.93)=3.54, p<0.005); the RER was higher in CSS than CON mice on each of days 17-20. Also during the light phase (Figure 2B) there was a group x day interaction effect (F(5, 108.06)=4.16, p<0.002), and RER was higher in CSS than CON mice on days 19 and 20.

(FIGURE 2 ABOUT HERE)

3.1.3 Spontaneous behaviors

Also in Expt 1, home cage behaviors were measured at four time points across each of CSS/CON days 4, 8 and 12. For self-grooming, there was a main effect of group (F(1, 22)=30.16, p<0.0001), with CSS mice self-grooming more than CON mice (Figure S2A). For sitting upright, there was a main effect of group (F(1, 22)=9.30, p<0.006), with CSS mice sitting upright more than CON mice (Figure S2B). These were the two specific behaviors for which a significant CSS effect was detected.

3.2 Effects of CSS on blood levels of glucose, plasma insulin and appetite hormones

In Experiment 2, in contrast to Expt 1, there was no significant difference in BW between CSS and CON mice across the 15-days (p=0.64, ANCOVA with baseline BW as covariate; Figure 3A). A fasting glucose tolerance test (GTT) was performed on the morning of CSS day 10 of the 15-day CSS procedure. For blood glucose (Figure 3B), when baseline (time -1 min) values were analyzed there was no difference between CSS and CON mice (p=0.43). There was a group x time interaction effect (ANCOVA: F(3.23, 67.91)=3.05, p<0.05); *post hoc* analysis identified that blood glucose was higher in CSS than CON mice at time 30 min (p<0.05). Blood glucose AUC was not different between groups for either Min -1 to 60 (p=0.20) or Min -1 to 120 (p=0.99) (Figure 3D). For fasting plasma insulin (Figure 3C), when baseline values were compared between groups, CSS mice had lower plasma insulin than CON mice (t(21)=2.86, p<0.01). In ANCOVA with baseline insulin as covariate, there was a group x time interaction effect (F(3.27, 62.16)=3.15, p<0.05); *post hoc* analysis identified that plasma insulin was lower in CSS than CON mice at time points 15 min (p<0.01) and 30 min (p<0.05) after glucose administration. Plasma insulin AUC was lower in CSS mice than CON mice at Min -1 to 60 (t(19)=4.21, p<0.001) and Min -1 to 120 (t(20)=3.55, p<0.01) (Figure 3E). For AUC with respect to increase above baseline, CSS mice had lower plasma insulin than CON mice at Min -1 to 60 (t(13)=2.33, p<0.05) but not at Min -1 to 120 (t(18)=1.85, p=0.08).

(FIGURE 3 ABOUT HERE)

In these same mice, in blood samples collected at 2 days post-CSS (day 17), the fasting plasma level of acylated ghrelin was significantly higher in CSS compared with CON mice ($t(19)=-2.23$, $p<0.05$, Figure 4A). There was no effect of CSS on fasting plasma leptin ($t(20)=1.62$, $p=0.11$, Figure 4B). However, in blood samples collected at 6 days post-CSS (day 21) in Expt 1, fasting plasma leptin was significantly lower in CSS compared with CON mice ($t(20)=5.97$, $p<0.001$, Figure 4C).

(FIGURE 4 ABOUT HERE)

3.3 Expression of appetite-hormone function genes in fat tissues and brain

In Expt 1, eWAT, iBAT and the brain were collected at 6 days post-CSS (day 21), and these tissues were studied with respect to expression of genes relevant to appetite-hormone function. In eWAT, there was a significant decrease in *Lep* expression in CSS mice compared with CON mice ($t(20)=-3.06$, $p<0.01$) (Figure 5A), and there was no CSS effect on the leptin receptor gene, *Lepr* ($p=0.92$) (Figure 5B). In iBAT, *Ucp-1* expression was increased in CSS mice compared with CON mice ($p<0.01$, Figure 5C). In brain regions of interest, *Ghs-r1a* and/or *Lepr* expression were quantified. For *Ghs-r1a* there was a significant increase in expression in the VMH in CSS compared with CON mice ($t(19)=2.92$, $p<0.05$) (Figure 5D); this was the only study brain region in which there was a CSS effect on *Ghs-r1a* expression. For *Lepr* there was no significant effect of CSS on expression in any study brain region (Figure 5E).

(FIGURE 5 ABOUT HERE)

3.4 Effects of CSS on glucose uptake by tissues measured using [^{18}F]FDG

In Expt 3, the effects of CSS on glucose utilization by the brain and peripheral tissues were studied 1 day post-CSS (day 16) by injecting [^{18}F]FDG and after 45 min measuring its biodistribution. For BW, there was a significant group x day-block interaction effect (ANOVA: $F(3, 33)=7.94$, $p<0.0001$), but in the absence of a CSS effect on BW in any specific day block, e.g. days -4 to 0: CON 28.2±1.12, CSS 28.8±1.7, $p=0.51$; days 11-15: CON 29.7±1.4, CSS 28.9±1.3, $p=0.30$. In one CSS mouse the [^{18}F]FDG uptake by whole brain was a high extreme outlier (greater than 3 times the interquartile range of the complete data set), and this mouse was excluded from the analysis. For whole brain, as well as for olfactory bulb, thalamus, midbrain and residual brain specifically, [^{18}F]FDG uptake was reduced in CSS relative to CON mice ($t(11) \geq 3.24$, $p<0.01$; Figure 6). For other brain regions and all peripheral tissues,

there was no significant effect of CSS on [^{18}F]FDG uptake ($p>0.04$; Figure 6 and supplementary Figure S3).

(FIGURE 6 ABOUT HERE)

4. Discussion

There is growing evidence that chronic stress impacts on individuals' energy status, and it is important to increase understanding of the relationships between peripheral and central effects. Here we conducted a study of the effects in mice of a chronic social stressor in terms of both peripheral and central energy-status measures and determinants. We were particularly interested in effects of potential relevance to the aetio-pathogenesis of human depression, for which chronic stress is a major risk factor and body weight loss is a common symptom. We conducted the study under the condition of a standard, low-fat diet; as well as being the diet used in our CSS studies to date, we expected that this would preclude adipose tissue increase, and thereby optimize the model's relevance to depression with body weight loss. A number of CSS effects on energy status and determinants thereof are demonstrated which together provide important insights into how energetic changes could potentially contribute to the symptoms and even the aetio-pathogenesis of depression.

In Expt 1, CSS mice had lower body weight than CON mice in the last 5 days of the 15-day stressor and the 5 days thereafter. This occurred despite CSS mice consuming the same amount of food as their CON counterparts, such that their body mass gain relative to cumulative food intake was lower. Chronic stress-induced reduced gain in BW relative to food intake can be manifested as either reduced BW gain despite similar food intake, or similar BW change despite increased food intake. For example, as in Expt 1, chronic subordinate-intruder stress led to a decrease in BW gain in the absence of an effect on food intake (Bartolomucci et al., 2004). Other studies have reported that chronic stress leads to a similar BW increase combined with increased food intake without e.g. 10-day CSD (Lutter et al., 2008; Kumar et al., 2013). Indeed, in our previous CSS studies the effect was a similar BW change combined with increased food intake in the CSS compared with CON mice (Bergamini et al., 2016; Kúkel'ová et al., 2018). In Expt 1 and in contrast to our previous studies, CON mice were singly caged rather than

as brother pairs and this could have acted as a mild stressor that increased feeding and, in the absence of CSS-specific effects, led to greater BW gain in CON mice.

The low BW of CSS mice in Expt 1co-occurred with reductions in epididymal white adipose tissue and interscapular brown adipose tissue. If the eWAT loss is representative of CSS-induced WAT loss in other body regions, this would be the major explanation for the CSS effect on BW; the BW profiles suggest that the loss of WAT began in the last 5 days of the 15-day CSS procedure. Stress-induced reduction in WAT has been observed previously. For example, mice exposed to chronic subordinate-intruder stress displayed a decrease in eWAT (Bartolomucci et al., 2004) and CSD mice displayed a decrease in overall WAT (Chuang et al., 2010). However, no change in eWAT was observed after a 24-day CSD procedure (Coccurello et al., 2017); these same mice exhibited an increase in iBAT, again in contrast to the decrease we observed in CSS mice. The present observed reduction in iBAT mass co-occurred with an apparently compensatory increase in *Ucp-1* expression in the remaining iBAT, suggesting that CSS effects on non-shivering thermogenesis were minimized (Morrison et al., 2014). However, during the earlier stages of the CSS protocol when we expect BAT deposits to be similar for both groups, we cannot rule out that increased expression of iBAT *Ucp-1* led to higher EE in CSS mice and contributed to their reduced weight gain. The expression of *Ucp-1* in WAT also has metabolic effects (Lizcano et al., 2019). We did not measure *Ucp-1* expression in WAT, however, and this is a limitation of the current study.

Energy expenditure was unchanged by CSS after controlling for BW. Taken together with the reduced gain in BW relative to food intake, this indicates that CSS mice were expending energy on processes other than BW maintenance/gain relative to CON mice. With regard to the nutrient source of expended energy, CSS mice had a respiratory exchange ratio value approaching 1; this is indicative of their energy-metabolism substrate comprising predominately carbohydrate rather than fat or protein, which in turn is commensurate with their low adipose-tissue levels (Arch et al., 2006). In CON mice, RER values were closer to 0.9 and commensurate with a more balanced energy source comprising fat and protein in addition to carbohydrate (Arch et al., 2006). In a CSD study in which mice were fed on a conventional diet and indirect calorimetry was conducted on day 18 of the 24-day stressor, whilst there was no stress effect on BW or food intake, the stressed mice did display greater EE relative to

CON mice (Coccurello et al., 2017). The mice were given 6 h habituation to the indirect calorimetry cage - considerably less than we deployed - and the increased EE in CSD mice might have reflected a more pronounced initial stress response to the test environment compared to control mice. There was no effect of CSD on RER in this study (Coccurello et al., 2017).

With regard to the causation of CSS-induced reduced BW gain relative to food intake, this could be attributable to one factor or a combination of several. These include: increased energy demand e.g. increased core body temperature, activation of the limbic brain-sympathetic autonomic nervous system pathway and elevated heart rate. Related to this, CSS mice did display higher spontaneous levels of self-grooming and upright sitting, behavioral changes that are consistent with an increased defensive state, and which would be expected to increase energy demand. Another putative causative factor would be decreased energy metabolism efficiency e.g. accumulation of mitochondrial fragmentation and damage (Picard et al., 2014). Finally, here, we would propose decreased energy intake efficiency: for example, stress-induced changes in microbiota can compromise energy absorption efficiency (Cani et al., 2019). Indeed, in a pilot study, CSS did alter the intestinal microbiota profile, with CSS mice displaying a reduction in *Akkermansia* spp, and increases in *Prevotella* spp., *Ruminococcus* spp., and *Lachnospiraceae* spp (supplementary Figure S4). The reduction in *Akkermansia* spp. is in accord with that described for 7-day CSD mice (McGaughey et al., 2019), and is particularly relevant here given that this bacteria genus is reduced in humans with glucose intolerance (Zhang et al., 2013) and exerts positive effects on glucose homeostasis (Depommier et al., 2019). Thus, the changes observed in the microbiota might well contribute to the CSS effects we observe on BW gain relative to food intake and EE, and on glucose metabolism; these latter CSS effects are discussed next.

In Expt 2, when mice were tested on day 10 of the CSS/CON procedure, overnight-fasted CSS mice had lower plasma levels of basal insulin than did CON mice. Whilst there was no difference between CSS and CON mice in basal blood glucose at this time point, when challenged with exogenous glucose (GTT), CSS mice had higher blood glucose at 30 min post-challenge. This was associated with a reduced plasma insulin AUC above baseline in the first hour post-glucose challenge, consistent with a relatively blunted insulin response to glucose. In CSD mice, when a GTT was conducted at 9 days post-CSD, blood glucose was also elevated at 30 min after challenge relative to CON mice, although

there was no CSD effect on basal insulin or insulin response to the GTT at this post-CSD stage (Van Der Kooij et al., 2018). The increased expression of iBAt *Ucp-1*, as observed in Expt 1, is typically associated with increased glucose uptake (e.g. Cannon et al.,2004); however, our Expt 2 findings suggest reduced glucose uptake at 30 min. We speculate that any effect of *Ucp-1* on glucose uptake is outweighed by other regulators of glucose homeostasis; in particular the substantial suppression of insulin we observed in the GTT.

With respect to the appetite hormone ghrelin, fasting plasma acylated ghrelin was increased in CSS mice, as has also been reported for CSD mice (Chuang et al., 2011; Lutter et al., 2008). Expression of the ghrelin receptor gene, *Ghs-r1a*, in the hypothalamic ventromedial nucleus (VMH) was also upregulated in CSS mice. Certain VMH neurons are responsive to both ghrelin and glucose (Routh et al., 2004; Li et al., 2017), and furthermore, ghrelin inhibits insulin secretion and increases RER (Tschöp et al., 2000; Müller et al., 2015). Therefore, the demonstrated CSS effects of increased ghrelin signaling, reduced plasma insulin and increased RER could be causally related. With regard to fasting leptin, this was unaffected (Expt 2) or reduced (Expt 1) by CSS; leptin levels were substantially higher in CON mice in Expt 1 compared with Expt 2. In a study conducted using ad libitum feeding we observed relatively high leptin in CON mice (similar to Expt 1) with a reduction in CSS mice (Bergamini et al., 2016). In contrast, in a study where mild food restriction was combined with operant testing for sweet reward, leptin was relatively low in CON mice and similar to that in CSS mice (Kúkel'ová et al., 2018). Integrating these findings with the present study suggests that in the latter, the effect of fasting in CON mice was greater in Expt 2 than in Expt 1. We also provide what to our knowledge is the first evidence that chronic stress induces downregulated expression of the leptin gene, *Lep*, in WAT; that is, eWAT mass was reduced and *Lep* expression per mass of remaining eWAT was also reduced, relative to CON mice. There was no effect of CSS on *Lepr* expression, neither in eWAT nor in the brain regions studied. The increases in plasma levels of ghrelin and gene expression of its receptor in VMH and the decreases in eWAT *Lep* expression and plasma leptin levels observed in CSS mice, are consistent with an increase in appetite and therefore daily food intake. Indeed, we have reported previously on such an increase in food intake to maintain a similar BW in CSS relative to CON mice (Bergamini et al., 2016; Kúkel'ová

et al., 2018). Nonetheless, it would have been advantageous for the interpretation of the current findings if we had also measured daily food intake in Expt 2, and this is a limitation of the present study.

The decrease in plasma insulin and increase in blood glucose in the GTT at day 10 of the 15-day CSS procedure, together with the high RER consistent with carbohydrate as the major substrate of energy metabolism at post-CSS days 17-20, is each consistent with an increased need for glucose in CSS mice. Relative to other organs and tissues, the CNS has a disproportionately high glucose need, due to the high energy requirement of neurons and glia (Mergenthaler et al., 2013). This certainly pertains in the mouse, although given its comparatively small relative brain-to-body size, not to the same extent as in relatively large-brained mammals and most notably humans, of course (Herculano-Houzel, 2011). Stress leads to marked increases in energy need and metabolism in the neural circuits for emotional-stimulus processing. However, chronic stress also leads to brain inflammation, oxidative stress and mitochondrial damage, such that CNS energy metabolism can become inefficient coincident with the very neurobehavioral state in which energy demand is high (Picard et al., 2014). Using induced metabolic bioluminescence imaging, recently it was demonstrated that CSD mice have high levels of brain glucose compared with controls (Van Der Kooij et al., 2018). Using [^{18}F]FDG positron emission tomography (PET), the same study demonstrated that CSD mice have lower CNS glucose uptake than control mice. This apparent paradox co-occurred with reduced membrane-protein levels of glucose transporter 1 (GluT1) in brain tissue (Van Der Kooij et al., 2018), suggesting that the observed CNS hyperglycemia was primarily extracellular and that this in turn led to attenuated active glucose transport across the blood-brain barrier (Van Der Kooij et al., 2018). By measuring [^{18}F]FDG uptake, here we corroborate the finding that chronic stress leads to attenuated CNS glucose utilization and also demonstrate that the brain is the only organ/tissue in which glucose utilization is significantly impacted by CSS. In [^{18}F]FDG uptake studies the amount of 2-FDG administered is low (< 5 nmol in the present study) and minimal compared to circulating glucose and the amount of glucose administered in the GTT. It is important to note that changes in the blood-brain barrier (BBB) could also contribute to this CSS effect, including changes in cerebral blood flow, capillary surface area, BBB glucose permeability and active glucose transport, and these will need to be investigated in a future study. One of the brain regions with decreased [^{18}F]FDG uptake in CSS mice was the midbrain, which includes the major

localizations of dopamine neuron cell bodies, namely ventral tegmental area and substantia nigra pars compacta. A previous study identified that CSS leads to attenuated mesolimbic dopamine activity (Bergamini et al., 2018), and this could be related to the decrease in glucose uptake. In depression, dynamic evaluation of cerebral glucose utilization by means of [^{18}F]FDG PET has identified evidence for reduced glucose uptake in prefrontal cortex and anterior cingulate cortex, two key regions in the neural networks that are impacted in depression (Price and Drevets, 2010; Videbech, 2000).

In summary therefore, using a standard diet and compared with controls, CSS mice displayed lower BW gain relative to food intake despite similar energy expenditure, reduced adipose tissue, increased carbohydrate contribution to energy substrate, and altered microbiota. These changes in energy status co-occurred with neuroendocrine changes signaling for increased food intake, namely reduced plasma insulin and leptin and increased plasma ghrelin and VMH ghrelin receptor expression. Importantly, however, whilst these CSS-induced changes are consistent with increased glucose metabolism, glucose utilization in the CNS was reduced. Disturbed glucose metabolism in the brain could represent an important explanatory link between the peripheral energy status changes observed in CSS mice in this study and the reduced interest in sweet-tasting food reward reported for CSS mice in previous studies (Bergamini et al., 2016; Kúkel'ová et al., 2018). This peripheral-CNS constellation displays similarity to the symptom combination of body weight loss and reduced interest in reward that is common in depression. It will now be important to utilize this model to further understanding of the mechanisms via which chronic stress can decrease brain glucose utilization and how this relates to regional and cellular changes in neural circuits for reward processing.

5. Acknowledgements

We are grateful to Björn Henz and Alex Osei for animal care, to Claudia Keller, Michaela Uebel and William Powell for their expert technical work, and to Dr. Maria Wiese, University of Copenhagen, Denmark, for help with the microbiota DNA sequencing and profiling. This research was carried out with the support of CNPq, the National Council for Scientific and Technological Development – Brazil, the Swiss National Science Foundation (grant 31003A_160147), and the University of Roehampton, London.

6. References

American Psychiatry Association, 2013. DSM-5 Diagnostic and statistical manual of mental disorders (5th ed.).

Arch, J.R.S., Hislop, D., Wang, S.J.Y., Speakman, J.R., 2006. Some mathematical and technical issues in the measurement and interpretation of open-circuit indirect calorimetry in small animals. Int. J. Obes. 30, 1322-1331. https://doi.org/10.1038/sj.ijo.0803280

Azzinnari, D., Sigrist, H., Staehli, S., Palme, R., Hildebrandt, T., Leparc, G., Hengerer, B., Seifritz, E., Pryce, C.R., 2014. Mouse social stress induces increased fear conditioning, helplessness and fatigue to physical challenge together with markers of altered immune and dopamine function. Neuropharmacology 85, 328–341. https://doi.org/10.1016/j.neuropharm.2014.05.039

Bali, A., Jaggi, A.S., 2016. An Integrative Review on Role and Mechanisms of Ghrelin in Stress, Anxiety and Depression. Curr. Drug Targets 17, 495-507. https://doi.org/10.2174/1389450116666150518095650

Bartolomucci, A., Pederzani, T., Sacerdote, P., Panerai, A.E., Parmigiani, S., Palanza, P., 2004. Behavioral and physiological characterization of male mice under chronic psychosocial stress. Psychoneuroendocrinology 29, 899–910. https://doi.org/10.1016/j.psyneuen.2003.08.003

Bergamini, G., Cathomas, F., Auer, S., Sigrist, H., Seifritz, E., Patterson, M., Gabriel, C., Pryce, C.R., 2016. Mouse psychosocial stress reduces motivation and cognitive function in operant reward tests: A model for reward pathology with effects of agomelatine. Eur. Neuropsychopharmacol. 26, 1448–1464. https://doi.org/10.1016/j.euroneuro.2016.06.009

Bergamini, G., Mechtersheimer, J., Azzinnari, D., Sigrist, H., Buerge, M., Dallmann, R., Freije, R., Kouraki, A., Opacka-Juffry, J., Seifritz, E., Ferger, B., Suter, T., Pryce, C.R., 2018. Chronic social stress induces peripheral and central immune activation, blunted mesolimbic dopamine function, and reduced reward-directed behaviour in mice. Neurobiology of Stress 8, 42-56. https://doi.org/10.1016/j.ynstr.2018.01.004

Bowe, J.E., Franklin, Z.J., Hauge-Evans, A.C., King, A.J., Persaud, S.J., Jones, P.M., 2014. Assessing glucose homeostasis in rodent models. J. Endocrinol. 222, 13–25. https://doi.org/10.1530/JOE-

14-0182

Cani, P.D., Van Hul, M., Lefort, C., Depommier, C., Rastelli, M., Everard, A., 2019. Microbial regulation of organismal energy homeostasis. Nat. Metab. 1, 34–46. https://doi.org/10.1038/s42255-018-0017-4

Cannon, B., Nedergaard, J., 2004. Brown adipose tissue: function and physiological significance. Physiol. Rev. 84, 277–359. https://doi.org/10.1152/physrev.00015.2003

Chuang, J.C., Krishnan, V., Yu, H.G., Mason, B., Cui, H., Wilkinson, M.B., Zigman, J.M., Elmquist, J.K., Nestler, E.J., Lutter, M., 2010. A β3-Adrenergic-Leptin-Melanocortin Circuit Regulates Behavioral and Metabolic Changes Induced by Chronic Stress. Biol. Psychiatry 67, 1075–1082. https://doi.org/10.1016/j.biopsych.2009.12.003

Chuang, J.C., Perelló, M., Sakata, I., Osborne-Lawrence, S., Savitt, J.M., Lutter, M., Zigman, J.M., 2011. Ghrelin mediates stress-induced food-reward behavior in mice. J. Clin. Invest. 121, 2684–2692. https://doi.org/10.1172/JCI57660

Coccurello, R., Romano, A., Giacovazzo, G., Tempesta, B., Fiore, M., Giudetti, A.M., Marrocco, I., Altieri, F., Moles, A., Gaetani, S., 2017. Increased intake of energy-dense diet and negative energy balance in a mouse model of chronic psychosocial defeat. Eur. J. Nutr. 57, 1485–1498. https://doi.org/10.1007/s00394-017-1434-y

Cong, W., Golden, E., Pantaleo, N., M. White, C., Maudsley, S., Martin, B., 2012. Ghrelin Receptor Signaling: A Promising Therapeutic Target for Metabolic Syndrome and Cognitive Dysfunction. CNS Neurol. Disord. - Drug Targets 9, 557-563. https://doi.org/10.2174/187152710793361513

Cummings, D.E., Purnell, J.Q., Frayo, R.S., Schmidova, K., Wisse, B.E., Weigle, D.S., 2001. A Preprandial Rise in Plasma Ghrelin Levels Suggests a Role in Meal Initiation in Humans. Diabetes 50, 1714–1719. https://doi.org/10.2337/diabetes.50.8.1714

Depommier, C., Everard, A., Druart, C., Plovier, H., Van Hul, M., Viera-Silva, S., Falony, G., Raes, J., Maiter, D., Delzenne, N.M., de Barsy, M., Loumaye, A., Hermans, M.P., Thissen, J.P., de Vos, W.M., Cani, P.D. 2019. Supplementation with Akkermansia muciniphila in overweight and obese human volunteers: a proof-of-concept exploratory study. Nat. Med. 25, 1096-1103. doi: 10.1038/s41591-019-0495-2

Farias, G., Netto, B.D.M., Bettini, S.C., Dâmaso, A.R., de Freitas, A.C.T., 2017. Neuroendocrine regulation of energy balance: Implications on the development and surgical treatment of obesity. Nutr. Health 23, 131-146. https://doi.org/10.1177/0260106017719369

Ferrannini, E., 1988. The theoretical bases of indirect calorimetry: a review. Metabolism 37, 287-301. https://doi.org/10.1016/0026-0495(88)90110-2

Friedman, J., 2014. 20 YEARS OF LEPTIN: Leptin at 20: an overview. J. Endocrinol. 223, T1-T8. https://doi.org/10.1530/joe-14-0405

Ge, J.F., Qi, C.C., Zhou, J.N., 2013. Imbalance of leptin pathway and hypothalamus synaptic plasticity markers are associated with stress-induced depression in rats. Behav. Brain Res. 249, 38–43. https://doi.org/10.1016/j.bbr.2013.04.020

Gordon, C.J., Becker, P., Ali, J.S., 1998. Behavioral thermoregulatory responses of single- and group-housed mice. Physiol. Behav. 65, 255-262. https://doi.org/10.1016/S0031-9384(98)00148-6

Grandjean, J., Azzinnari, D., Seuwen, A., Sigrist, H., Seifritz, E., Pryce, C.R., Rudin, M., 2016. Chronic psychosocial stress in mice leads to changes in brain functional connectivity and metabolite levels comparable to human depression. NeuroImage 142, 544-552. http://dx.doi.org/10.1016/j.neuroimage.2016.08.013

Harper, D.G., Jensen, J.E., Ravichandran, C., Perlis, R.H., Fava, M., Renshaw, P.F., Iosifescu, D. V., 2017. Tissue Type-Specific Bioenergetic Abnormalities in Adults with Major Depression. Neuropsychopharmacology 42, 876-885. https://doi.org/10.1038/npp.2016.180

Harris, R.B.S., 2014. Chronic and acute effects of stress on energy balance: are there appropriate animal models? Am. J. Physiol. Integr. Comp. Physiol. 308, R250-R265. https://doi.org/10.1152/ajpregu.00361.2014

Herculano-Houzel, S., 2011. Scaling of brain metabolism with a fixed energy budget per neuron: Implications for neuronal activity, plasticity and evolution. PLoS One. 6, e17514. https://doi.org/10.1371/journal.pone.0017514

Joung, K.E., Park, K.H., Zaichenko, L., Sahin-Efe, A., Thakkar, B., Brinkoetter, M., Usher, N., Warner, D., Davis, C.R., Crowell, J.A., Mantzoros, C.S., 2014. Early life adversity is associated with elevated levels of circulating leptin, irisin, and decreased levels of adiponectin in midlife adults.

J. Clin. Endocrinol. Metab. 99, E1055-1060. https://doi.org/10.1210/jc.2013-3669

Kan, C., Silva, N., Golden, S.H., Rajala, U., Timonen, M., Stahl, D., Ismail, K., 2013. A systematic review and meta-analysis of the association between depression and insulin resistance. Diabetes Care 36, 480-489. Htpps://doi: 10.2337/dc12-1442.

Kessler, R.C., 1997. The effects of stressful life events on depression. Annu. Rev. Psychol. 48, 191-214. https://doi.org/10.1146/annurev.psych.48.1.191

Krishnan, V., Han, M.-H.H., Graham, D.L., Berton, O., Renthal, W., Russo, S.J., LaPlant, Q., Graham, A., Lutter, M., Lagace, D.C., Ghose, S., Reister, R., Tannous, P., Green, T.A., Neve, R.L., Chakravarty, S., Kumar, A., Eisch, A.J., Self, D.W., Lee, F.S., Tamminga, C.A., Cooper, D.C., Gershenfeld, H.K., Nestler, E.J., 2007. Molecular Adaptations Underlying Susceptibility and Resistance to Social Defeat in Brain Reward Regions. Cell 131, 391–404. https://doi.org/10.1016/j.cell.2007.09.018

Kúkel'ová, D., Bergamini, G., Sigrist, H., Seifritz, E., Hengerer, B., Pryce, C.R., 2018. Chronic social stress leads to reduced gustatory reward salience and effort valuation in mice. Front. Behav. Neurosci. https://doi.org/10.3389/fnbeh.2018.00134

Kumar, J., Chuang, J.C., Na, E.S., Kuperman, A., Gillman, A.G., Mukherjee, S., Zigman, J.M., McClung, C.A., Lutter, M., 2013. Differential effects of chronic social stress and fluoxetine on meal patterns in mice. Appetite 64, 81–88. https://doi.org/10.1016/j.appet.2012.12.023

Li, B., Zhuang, Q.X., Gao, H.R., Wang, J.J., Zhu, J.N., 2017. Medial cerebellar nucleus projects to feeding-related neurons in the ventromedial hypothalamic nucleus in rats. Brain Struct. Funct. 222, 957-971. https://doi.org/10.1007/s00429-016-1257-2

Lizcano, F., 2019. The beige adipocyte as a therapy for metabolic diseases. Int. J. Mol. Sci. 20, E5058. https://doi.org/10.3390/ijms20205058

Lu, X.Y., 2007. The leptin hypothesis of depression: a potential link between mood disorders and obesity? Curr. Opin. Pharmacol. 7, 648-652. https://doi.org/10.1016/j.coph.2007.10.010

Lutter, M., Sakata, I., Osborne-Lawrence, S., Rovinsky, S.A., Anderson, J.G., Jung, S., Birnbaum, S., Yanagisawa, M., Elmquist, J.K., Nestler, E.J., Zigman, J.M., 2008. The orexigenic hormone ghrelin defends against depressive symptoms of chronic stress. Nat. Neurosci. 11, 752–753.

https://doi.org/10.1038/nn.2139

Martin, P., Bateson, P., 2007. Measuring Behaviour. An Introductory Guide, third ed.. Cambridge University Press, Cambridge.

McGaughey, K.D., Yilmaz-Swenson, T., Elsayed, N.M., Cruz, D.A., Rodriguiz, R.M., Kritzer, M.D., Peterchev, A.V., Roach, J., Wetsel, W.C., Williamson, D.E. 2019. Relative abundance of *akkermansia* spp. and other bacterial phylotypes correlates with anxiety- and depressive-like behavior following social defeat in mice. Sci. Reports 9, 3281. https://doi.org/10.1038/s41598-019-40140-5

Mergenthaler, P., Lindauer, U., Dienel, G.A., Meisel, A., 2013. Sugar for the brain: The role of glucose in physiological and pathological brain function. Trends Neurosci. 36, 587–597. https://doi.org/10.1016/j.tins.2013.07.001

Moles, A., Bartolomucci, A., Garbugino, L., Conti, R., Caprioli, A., Coccurello, R., Rizzi, R., Ciani, B., D'Amato, F.R., 2006. Psychosocial stress affects energy balance in mice: Modulation by social status. Psychoneuroendocrinology 31, 623–633. https://doi.org/10.1016/j.psyneuen.2006.01.004

Morrison, S.F., Madden, C.J., Tupone, D., 2014. Central neural regulation of brown adipose tissue thermogenesis and energy expenditure. Cell Metab. 19, 741-756. https://doi.org/10.1016/j.cmet.2014.02.007

Müller, T.D., Nogueiras, R., Andermann, M.L., Andrews, Z.B., Anker, S.D., Argente, J., Batterham, R.L., Benoit, S.C., Bowers, C.Y., Broglio, F., Casanueva, F.F., D'Alessio, D., Depoortere, I., Geliebter, A., Ghigo, E., Cole, P.A., Cowley, M., Cummings, D.E., Dagher, A., Diano, S., Dickson, S.L., Diéguez, C., Granata, R., Grill, H.J., Grove, K., Habegger, K.M., Heppner, K., Heiman, M.L., Holsen, L., Holst, B., Inui, A., Jansson, J.O., Kirchner, H., Korbonits, M., Laferrère, B., LeRoux, C.W., Lopez, M., Morin, S., Nakazato, M., Nass, R., Perez-Tilve, D., Pfluger, P.T., Schwartz, T.W., Seeley, R.J., Sleeman, M., Sun, Y., Sussel, L., Tong, J., Thorner, M.O., van der Lely, A.J., van der Ploeg, L.H.T., Zigman, J.M., Kojima, M., Kangawa, K., Smith, R.G., Horvath, T.L., Tschöp, M.H., 2015. Ghrelin. Mol. Metab. 4, 437–460. https://doi.org/10.1016/j.molmet.2015.03.005

Paxinos, G., Franklin, K.B.J., 2004. The mouse brain in stereotaxic coordinates, Academic Press.

https://doi.org/10.1016/S0306-4530(03)00088-X

Picard, M., Juster, R.P., McEwen, B.S., 2014. Mitochondrial allostatic load puts the “gluc” back in glucocorticoids. Nat. Rev. Endocrinol. 10, 303-310. https://doi.org/10.1038/nrendo.2014.22

Price, J.L., Drevets, W.C., 2010. Neurocircuitry of mood disorders. Neuropsychopharmacology 35, 192-216. https://doi.org/10.1038/npp.2009.104

Razzoli, M., Carboni, L., Andreoli, M., Ballottari, A., Arban, R., 2011a. Different susceptibility to social defeat stress of BalbC and C57BL6/J mice. Behav. Brain Res. 2016, 100–108. https://doi.org/10.1016/j.bbr.2010.07.014

Routh, V.H., Song, Z., Liu, X., 2004. The role of glucosensing neurons in the detection of hypoglycemia. Diabetes Technol. Ther. 6, 413-421. https://doi.org/10.1089/152091504774198133

Sanghez, V., Razzoli, M., Carobbio, S., Campbell, M., McCallum, J., Cero, C., Ceresini, G., Cabassi, A., Govoni, P., Franceschini, P., de Santis, V., Gurney, A., Ninkovic, I., Parmigiani, S., Palanza, P., Vidal-Puig, A., Bartolomucci, A., 2013. Psychosocial stress induces hyperphagia and exacerbates diet-induced insulin resistance and the manifestations of the Metabolic Syndrome. Psychoneuroendocrinology 38, 2933–2942. https://doi.org/10.1016/j.psyneuen.2013.07.022

Sephton, S.M., Herde, A.M., Mu, L., Keller, C., Rüdisühli, S., Auberson, Y., Schibli, R., Krämer, S.D., Ametamey, S.M., 2015. Preclinical evaluation and test–retest studies of [18F]PSS232, a novel radioligand for targeting metabotropic glutamate receptor 5 (mGlu5). Eur. J. Nucl. Med. Mol. Imaging 42, 128-137. https://doi.org/10.1007/s00259-014-2883-7

Simmons, W.K., Burrows, K., Avery, J.A., Kerr, K.L., Taylor, A., Bodurka, J., Potter, W., Teague, T.K., Drevets, W.C., 2018. Appetite changes reveal depression subgroups with distinct endocrine, metabolic, and immune states. Mol. Psychiatry. https://doi.org/10.1038/s41380-018-0093-6

Torres, S.J., Nowson, C.A., 2007. Relationship between stress, eating behavior, and obesity. Nutrition 23, 887–894. https://doi.org/10.1016/j.nut.2007.08.008

Tschöp, M.H., Smiley, D.L., Heiman, M.L., 2000. Ghrelin induces adiposity in rodents. Nature 407, 908–913. https://doi.org/10.1038/35038090

Tschöp, M.H., Speakman, J.R., Arch, J.R., Auwerx, J., Bruning, J.C., Chan, L., Eckel, R.H., Farese, R.V., Jr., Galgani, J.E., Hambly, C., Herman, M.A., Horvath, T.L., Kahn, B.B., Kozma, S.C., Maratos-Flier, E., Muller, T.D., Munzberg, H., Pfluger, P.T., Plum, L., Reitman, M.L., Rahmouni, K., Shulman, G.I., Thomas, G., Kahn, C.R., Ravussin, E., 2011. A guide to analysis of mouse energy metabolism. Nat Methods 9, 57-63. https:// doi: 10.1038/nmeth.1806

Van Der Kooij, M.A., Jene, T., Treccani, G., Miederer, I., Hasch, A., Voelxen, N., Walenta, S., Müller, M.B., 2018. Chronic social stress-induced hyperglycemia in mice couples individual stress susceptibility to impaired spatial memory. Proc. Natl. Acad. Sci. U. S. A. 115, E10187-E10196. https://doi.org/10.1073/pnas.1804412115

Videbech, P., 2000. PET measurements of brain glucose metabolism and blood flow in major depressive disorder: A critical review. Acta Psychiatr. Scand. 101, 11-20. https://doi.org/10.1034/j.1600-0447.2000.101001011.x

Willner, P., 2017. The chronic mild stress (CMS) model of depression: History, evaluation and usage. Neurobiol. Stress 6, 78–93. https://doi.org/10.1016/j.ynstr.2016.08.002

Zhang, X., Shen, D., Fang, Z., Jie, Z., Qiu, X., Zhang, C., Chen, Y., Ji, L. 2013. Human gut microbiota changes reveal the progression of glucose intolerance. PLoS One 8, e71108. https:// 10.1371/journal.pone.0071108

FIGURE LEGENDS

Figure 1. Effects of 15-day chronic social stress (CSS, N=12) versus control handling (CON, N=12) on body weight, food intake and adipose tissue mass (Expt 1). (A) Absolute body weight. (B) Daily food intake. Values are overall means +/- standard deviation per 5-day block. *p≤0.05, **p≤0.01 for CSS versus CON mice following group x day block interaction in ANCOVA and day block-specific post hoc LSD testing. (C) Change in body weight relative to food intake. (D) Mass of epididymal WAT. (E) Mass of interscapular BAT. For A-B, values are means +/- SD. For C-E, individual values and group means are shown; *p≤0.05, ***p≤0.001 for CSS versus CON mice in independent sample *t*-tests. Sample size differences are due to removal of statistical outlier values.

Figure 2. Effects of 15-day chronic social stress (CSS, N=12) versus control handling (CON, N=12) on energy status as measured using indirect calorimetry (Expt 1). (A) Energy expenditure. (B) Respiratory exchange ratio. Each value is the overall group mean +/- standard deviation per day and phase (dark/active, light/inactive). Statistical analysis was conducted using mixed model ANCOVA with baseline BW as covariate for EE and mixed model ANOVA for RER, based on data obtained on days -1, 0, 17, 18, 19, 20. Values are means +/- SD; *p≤0.05, **p≤0.01, ***p≤0.001, for CSS versus CON mice following a significant group x day interaction effect and subsequent day-specific post hoc tests with Bonferroni correction.

Figure 3. Effects of the chronic social stress procedure (CSS, N=12) versus control handling (CON, N=12) on levels of blood glucose and plasma insulin at day 10 (Expt 2). (A) Body weight. Although there was a significant group x day block interaction in ANCOVA, there was no significant post hoc group difference at any specific day block. (B) Blood glucose levels across the GTT sampling period. *p≤0.05 for CSS versus CON mice following significant group x sampling time interaction in ANOVA and LSD *post hoc* testing. (C) Plasma insulin levels across the GTT sampling period. *p≤0.05, **p≤0.01 for CSS versus CON mice following group x sampling time interaction in ANCOVA and LSD *post hoc* testing. (D) Blood glucose total area under the curve at Min -1 to 60 and Min -1 to 120. (E) Plasma insulin total area under the curve calculated from 0 at Min -1 to 60 and Min -1 to 120. For A-C, values are means +/- SD. For D–E, individual values and group means are shown; *p≤0.05, ***p≤0.001 for CSS versus CON mice analyzed by independent Student's t-tests. Sample size differences are due to removal of statistical outlier values.

Figure 4. Effects of 15-day chronic social stress (CSS, N=12) versus control handling (CON, N=12) on plasma levels of appetite hormones. (A) Acylated ghrelin at day 17 (Expt 2). (B) Leptin at day 17 (Expt 2). (C) Leptin at day 21 (Expt 1). Individual values and group means are shown. *p≤0.05, ***p≤0.001 for CSS versus CON mice analyzed by independent Student`s *t*-test. Sample size differences are due to removal of statistical outlier values.

Figure 5. Effects of 15-day chronic social stress (CSS, N=12) versus control handling (CON, N=12) on expression of genes relevant to appetite hormone function in adipose tissue and brain collected on day 21 (Expt 1). In epididymal white adipose tissue: (A) Leptin, *Lep*. (B) Leptin receptor, *Lepr*. In

interscapular brown adipose tissue: (C) Uncoupling protein 1, *Ucp-1*. In specific brain regions: (D) Ghrelin receptor, *Ghr-r1a*. (E) *Lepr*. Values are fold change + SEM. **p≤0.01, ***p≤0.001 for CSS versus CON mice analyzed by independent Student's *t*-test. Abbreviations: mPFC, medial prefrontal cortex; NAcc, nucleus accumbens; PVN, paraventricular nucleus; ARC, arcuate nucleus; VMH, ventromedial nucleus; VTA, ventral tegmental area.

Figure 6. Effects of 15-day chronic social stress (CSS, N=6) versus control handling (CON, N=7) on ex vivo biodistribution of [^{18}F] FDG in tissue from specific brain regions at 45 minutes post-injection (Expt 3). For (A) whole brain and (B)-(F) selected brain regions, the accumulated radioactivity was expressed as percentage normalised (MBq/kg BW) injected dose per gram of tissue. (G) Sagittal image with Nissl staining at level 1.08 mm lateral to midline, showing the location of brain regions that were sampled for the data presented in figures (B)-(F). Figure from G. Paxinos and KBJ Franklin (2001) The Mouse Brain in Stereotaxic Coordinates. Academic Press. Reprinted with permission of Elsevier. Individual values and group means are shown; **p<0.01 and (*) p<0.05 in independent Student's *t*-tests, with p<0.01 used for statistical significance as an adjustment for multiple testing (see also Figure S3).

FIGURE 1

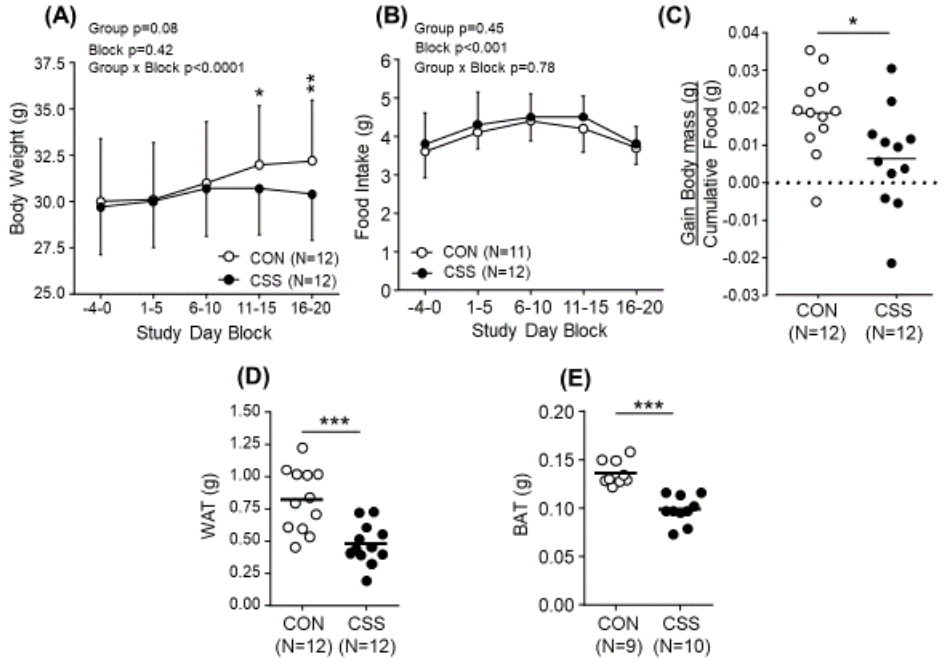
(A)
Group p=0.08
Block p=0.42
Group x Block p<0.0001
Body Weight (g)
CON (N=12)
CSS (N=12)
-4-0
1-5
6-10
11-15
16-20
Study Day Block
(B)
Group p=0.45
Block p<0.001
Group x Block p=0.78
Food Intake (g)
CON (N=11)
CSS (N=12)
Study Day Block
(C)
Gain Body mass (g)
Cumulative Food (g)
CON (N=12)
CSS (N=12)
(D)
WAT (g)
CON (N=12)
CSS (N=12)
(E)
BAT (g)
CON (N=9)
CSS (N=10)

FIGURE 2

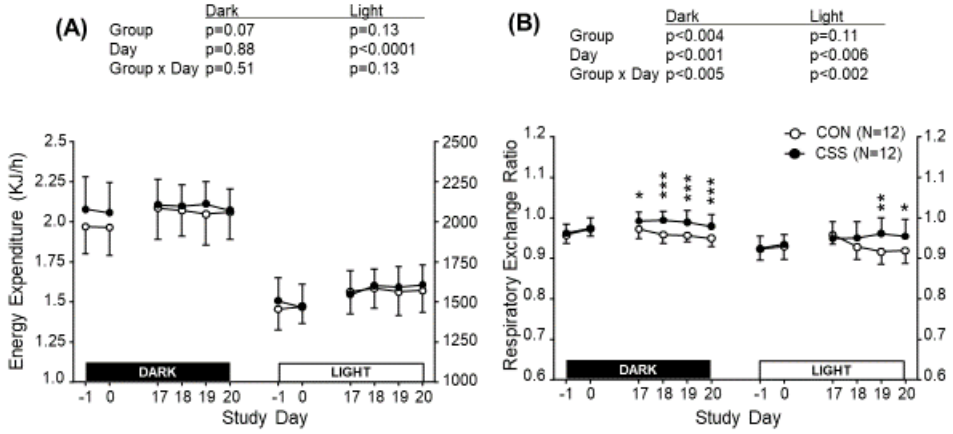
(A)
Dark
Light
Group p=0.07 p=0.13
Day p=0.88 p<0.0001
Group x Day p=0.51 p=0.13
(B)
Dark
Light
Group p<0.004 p=0.11
Day p<0.001 p<0.006
Group x Day p<0.005 p<0.002
Energy Expenditure (KJ/h)
Respiratory Exchange Ratio
CON (N=12)
CSS (N=12)
DARK
LIGHT
Study Day
-1 0 17 18 19 20 -1 0 17 18 19 20

FIGURE 3

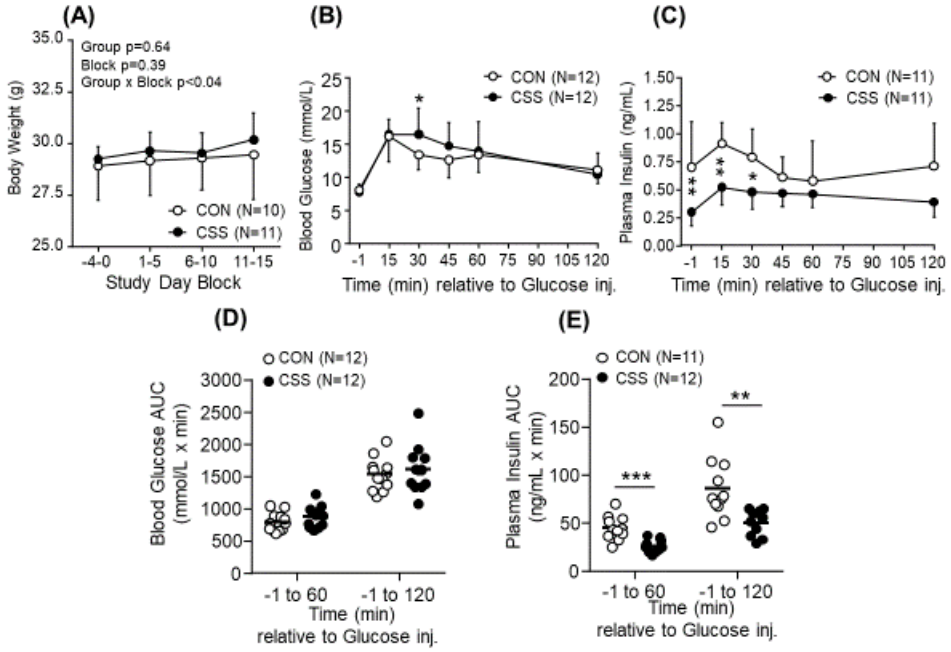
(A)
Group p=0.64
Block p=0.39
Group x Block p<0.04
Body Weight (g)
CON (N=10)
CSS (N=11)
-4-0
1-5
6-10
11-15
Study Day Block
(B)
Blood Glucose (mmol/L)
CON (N=12)
CSS (N=12)
Time (min) relative to Glucose inj.
(C)
Plasma Insulin (ng/mL)
CON (N=11)
CSS (N=11)
Time (min) relative to Glucose inj.
(D)
Blood Glucose AUC (mmol/L x min)
CON (N=12)
CSS (N=12)
-1 to 60
-1 to 120
Time (min) relative to Glucose inj.
(E)
Plasma Insulin AUC (ng/mL x min)
CON (N=11)
CSS (N=12)
-1 to 60
-1 to 120
Time (min) relative to Glucose inj.

FIGURE 4

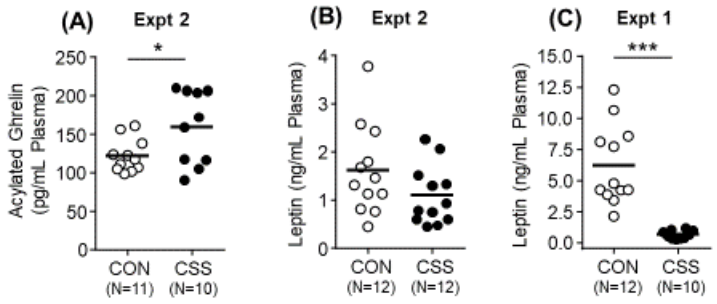
(A)
Expt 2
*
Acylated Ghrelin (pg/mL Plasma)
250
200
150
100
50
0
CON (N=11)
CSS (N=10)
(B)
Expt 2
Leptin (ng/mL Plasma)
4
3
2
1
0
CON (N=12)
CSS (N=12)
(C)
Expt 1
***
Leptin (ng/mL Plasma)
15.0
12.5
10.0
7.5
5.0
2.5
0.0
CON (N=12)
CSS (N=10)

FIGURE 5

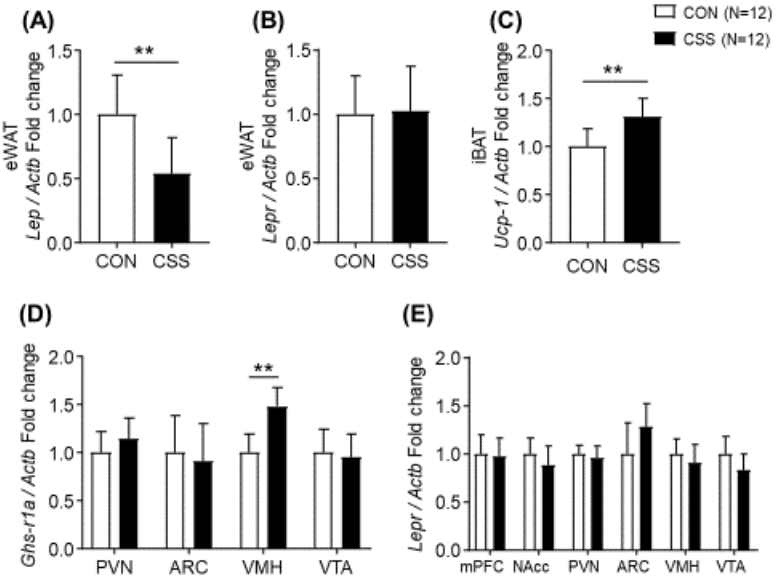
(A)
eWAT
Lep / Actb Fold change
1.5
1.0
0.5
0.0
**
CON
CSS
(B)
eWAT
Lepr / Actb Fold change
1.5
1.0
0.5
0.0
CON
CSS
(C)
CON (N=12)
CSS (N=12)
iBAT
Ucp-1 / Actb Fold change
2.0
1.5
1.0
0.5
0.0
**
CON
CSS
(D)
Ghs-r1a / Actb Fold change
2.0
1.5
1.0
0.5
0.0
**
PVN
ARC
VMH
VTA
(E)
Lepr / Actb Fold change
2.0
1.5
1.0
0.5
0.0
mPFC
NAcc
PVN
ARC
VMH
VTA

FIGURE 6

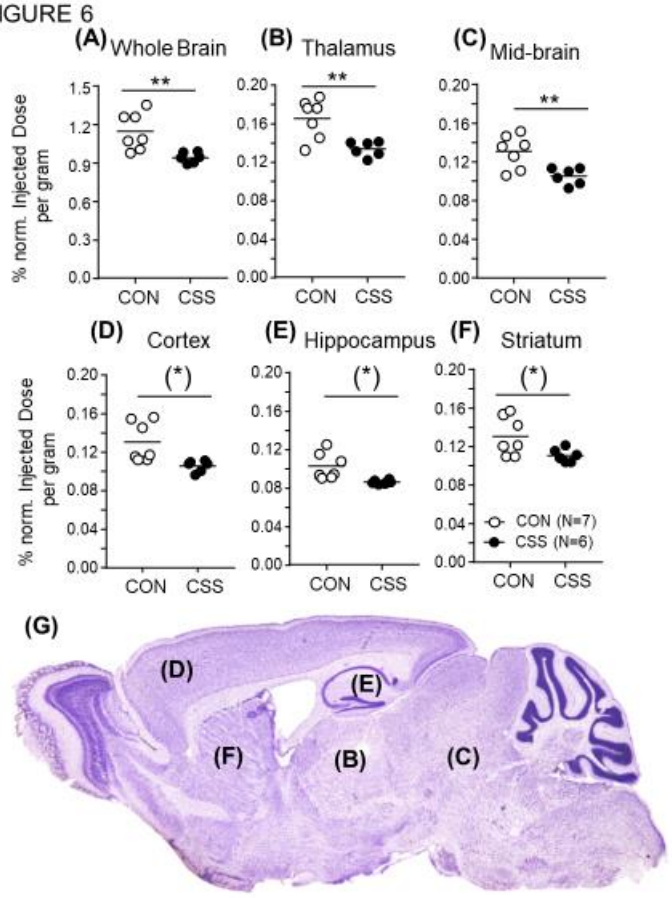
(A) Whole Brain
(B) Thalamus
(C) Mid-brain
(D) Cortex
(E) Hippocampus
(F) Striatum
% norm. Injected Dose per gram
**
(*)
CON
CSS
CON (N=7)
CSS (N=6)
(G)
(D)
(E)
(F)
(B)
(C)

Supplementary Table and Figures

Table S1. List of primer sequences and PCR conditions used

Gene	Primer sequence ('5 – 3')	PCR product (bp)	Annealing Temp. (°C)	Extension (sec)	PCR *E* (%)
Ucp-1	FW: CTGCCAGGACAGTACCCAAG RV: GACCCGAGTCGCAGAAAAGA	110	63	40	100
Lep	FW: TTTCACACACGCAGTCGGTA RV: GCACATTTTGGGAAGGCAGG	150	63	40	96
Lepr	FW: TTTCACACACGCAGTCGGTA RV: GCACATTTTGGGAAGGCAGG	138	60	30	109
Ghs-r1a	FW: ACAAACAGACAGTGAAGATG RV: TGTAGAGAATGGGGTTGATG	197	60	30	102
Actb	FW: GGCTGTATTCCCCTCCATCG RV: CCAGTTGGTAACAATGCCATGT	154	63	30	103

Abbreviations: *Actb,* actin, beta; *Ghs-r1a,* growth hormone secretagogue receptor; *Lep,* leptin; *Lepr,* leptin receptor; *Ucp-1,* uncoupling protein 1.

The PCR cycle conditions used were 5 min at 95˚C, 10 sec at 95˚C, and the following annealing conditions specific to each target: *Ucp-1* (63˚C, 40s), *Lep* (63˚C, 40s), *Lepr* (60˚C, 30s), *Ghs-r1a* (60˚C, 30s), *Actb* (63˚C, 30s). A melting curve was run for each PCR plate.

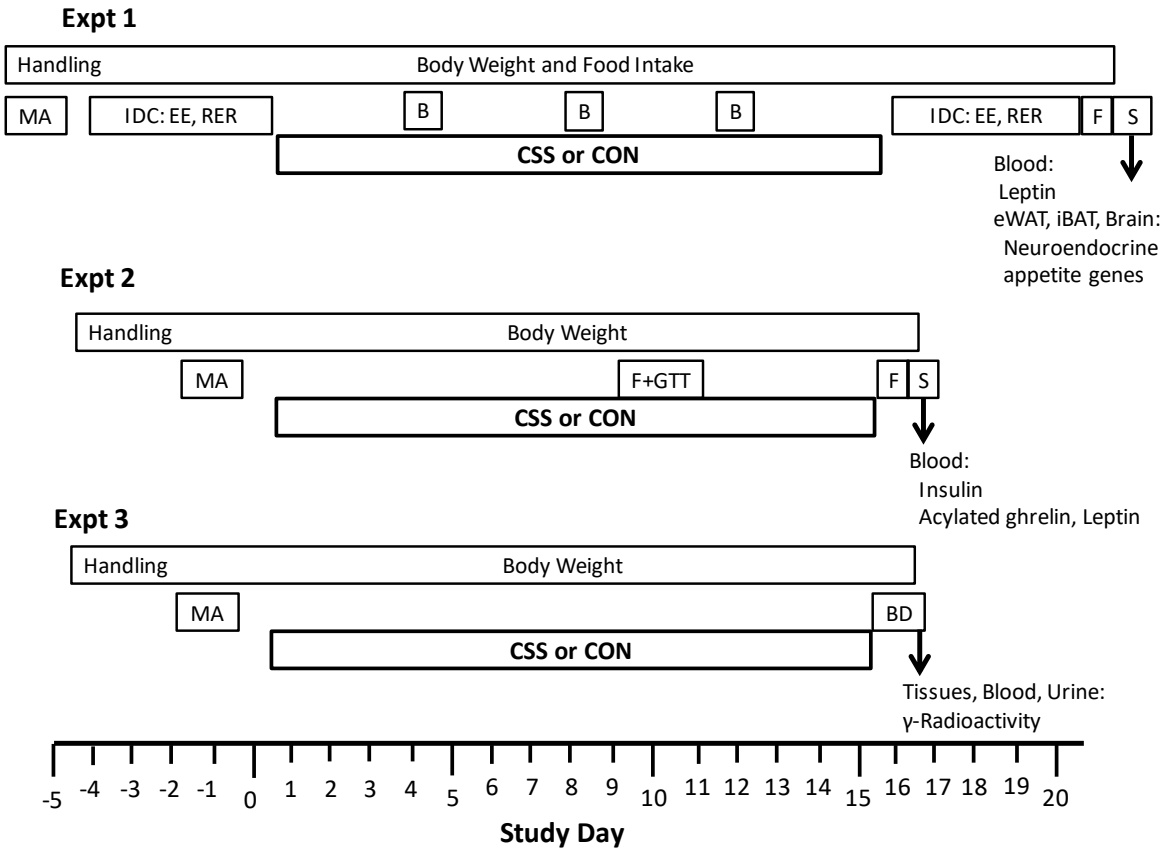

Figure S1. Experimental designs. Three experiments were conducted with mice exposed to chronic social stress (CSS) or control handling (CON) on days 1-15. Mice were handled at the onset of experiments and body weights were measured daily. Mice were given a motor activity test (MA), and allocation to CSS and CON groups was counterbalanced according to activity and body weight. **Experiment 1:** On days -4 to 0 mice were placed in indirect calorimetry cages for measurement of baseline energy expenditure and respiratory exchange ratio (IDC: EE, RER). Behavioral observations (B) were conducted on days 4, 8 and 12 of the CSS/CON procedure. On days 16-20 post-CSS/CON IDC: EE, RER was conducted. Overnight on day 20/21 mice underwent F followed on day 21 by S with collection of trunk blood, fat tissue and brain. **Experiment 2:** Overnight on day 9/10 of CSS/CON procedure, mice were fasted (F) and on morning of day 10 a glucose tolerance test with repeated blood sampling for glucose and insulin determinations (GTT) was conducted. Overnight on day 16/17 mice underwent F followed on day 17 by sacrifice (S) with trunk blood sampling for insulin and ghrelin determination. **Experiment 3:** On day 16, to assess glucose biodistribution (BD), mice were injected with [^{18}F]FDG and after 45 min trunk blood, urine and tissue samples were collected for determination of accumulated radioactivity.

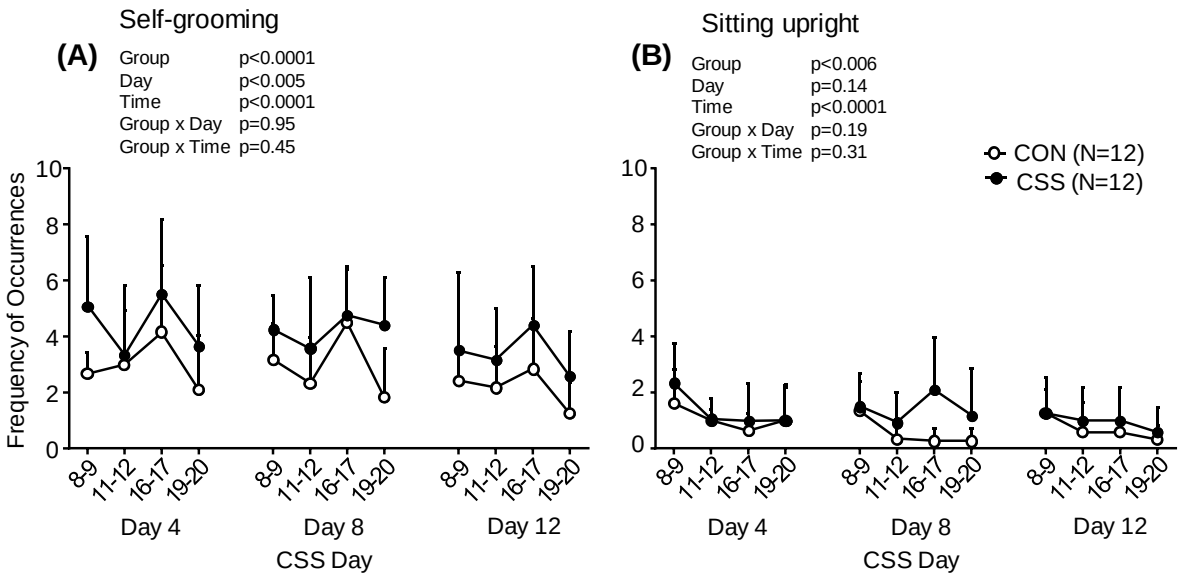

Figure S2. Effects of the CSS procedure on home cage behavior. (A) Self-grooming. (B) Sitting upright. Values are mean + standard deviation, N=12 per group. P values are for ANOVA with factors group, day and time of day.

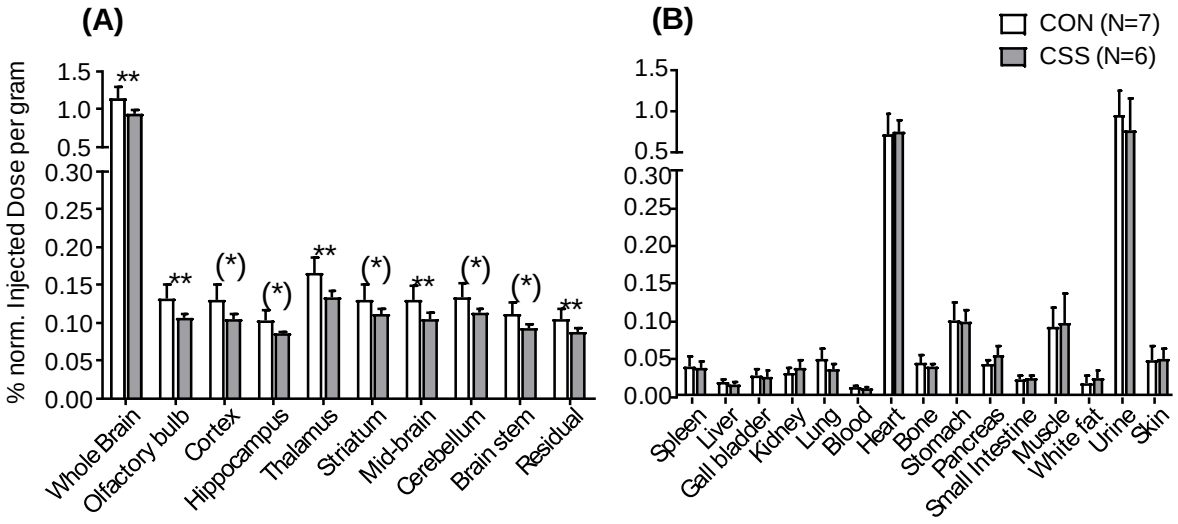

Figure S3. Ex vivo biodistribution of [^{18}F]FDG in (A) brain tissues and (B) body tissues and compartments at 45 minutes after injection. For each tissue, the accumulated radioactivity was expressed as percentage normalized (MBq/kg BW) injected dose per gram of tissue. ** $p<0.01$ and (*) $p<0.05$ in independent Student's *t*-tests; significance was set at $p<0.01$ to compensate for multiple testing.

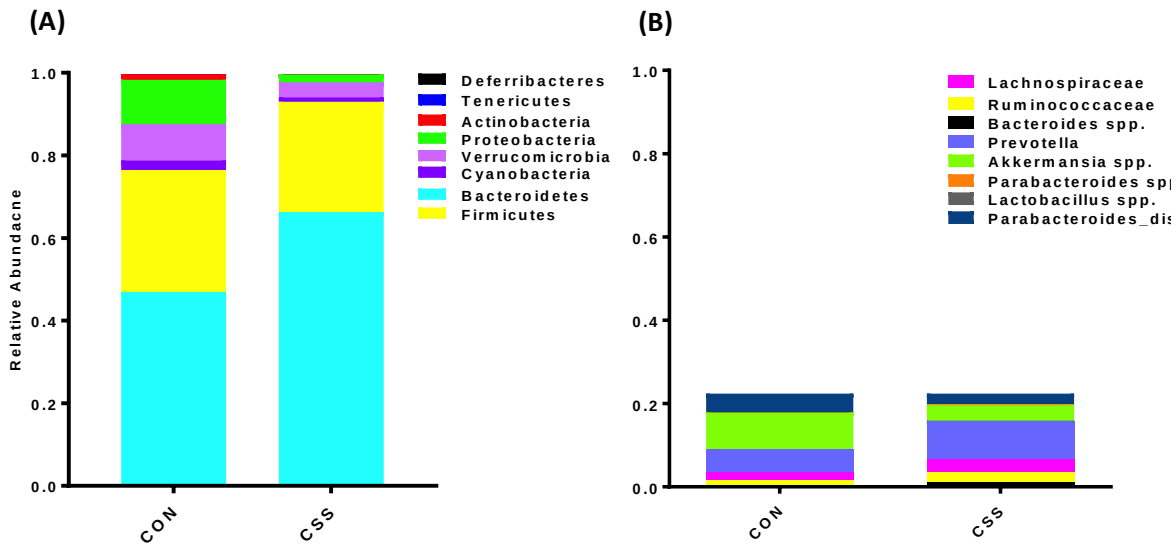

Figure S4. Phylum-Genus level relative abundance profiles of gut-derived microbial communities in chronic social stress (CSS) and control (CON) mice. (A) Relative abundance of bacterial communities at the phylum taxonomic rank. (B) Representative graphs of relative abundance of bacterial communities at the genus taxonomic rank. At day 15, fresh-voided faeces were collected from CSS (n=12) and CON (n=12) mice and total DNA was extracted for 16S rRNA gene-based next-generation sequencing. The V3-V4 hypervariable region of the 16S rRNA gene was PCR-amplified using the primer set 341F/805R. PCR products of about 460 bp were purified using a magnetic bead-based system (Agencourt AMPure XP; Beckman Coulter, Brea, CA) and indexed by limited-cycle PCR using Nextera technology (Illumina, San Diego, CA). Indexed libraries, further cleaned up as described above, were pooled at equimolar concentration, denatured and diluted to 6 pmol/l. Sequencing was performed on an Illumina MiSeq platform using the 2×250 bp protocol, according to the manufacturer's instructions. Sequencing reads were deposited in the National Center for Biotechnology Information Sequence Read Archive (NCBI SRA; BioProject ID PRJNA592433). CSS mice displayed a significant increase in *Bacteroides* spp. numbers compared to CON mice ($p<0.05$), with phyla in lower abundance including Proteobacteria, Firmicutes and Verrucomicrobia. At genus level, CSS mice displayed a significant decrease in *Akkermansia* spp. ($p<0.05$), and increases in *Prevotella* spp., *Ruminococcus* spp. and *Lachnospiraceae* spp.